Eur. Phys. J. D **23**, 351–357 (2003)
DOI: 10.1140/epjd/e2003-00071-3

THE EUROPEAN PHYSICAL JOURNAL D

Effect of melting on ionization potential of sodium clusters

A. Rytkönen[a] and M. Manninen

Department of Physics, University of Jyväskylä, P.O. Box 35 (YFL), 40014 University of Jyväskylä, Finland

Received 1st November 2002
Published online 24 April 2003 –

Abstract. The effect of melting transition on the ionization potential has been studied for sodium clusters with 40, 55, 142, and 147 atoms, using *ab initio* and classical molecular dynamics. Classical and *ab initio* simulations were performed to determine the ionization potential of Na_{142} and Na_{147} for solid, partly melted, and liquid structures. The results reveal no correlation between the vertical ionization potential and the degree of surface disorder, melting, or the total energy of the cluster obtained with the *ab initio* method. However, in the case of 40 and 55 atom clusters, the ionization potential seems to decrease when the cluster melts.

PACS. 36.40.Cg Electronic and magnetic properties of clusters – 36.40.Ei Phase transitions in clusters

1 Introduction

The melting behavior of metal clusters has been intensively discussed during the last decade. A recently developed experimental method has been successfully applied to determine the melting temperatures of sodium clusters with from 55 to 339 atoms [1]. The size dependence of the melting temperature contained features explainable in terms of neither geometric nor electronic magic numbers. This suggests that the melting temperature of small metal cluster depends on its geometry and electronic structure in a complicated way.

Experimental studies on melting have been performed also for large metal clusters. Martin *et al.* [2] determined the melting temperatures of sodium clusters with from 923 to 10 179 atoms by observing the disappearance of the geometric shell structure in the mass spectra of clusters as their temperature was raised. Sodium clusters with adjustable temperature were ionized with light the wavelength of which was chosen so that the photon energy corresponds to the ionization threshold of the sodium cluster. At low temperatures, the mass spectrum showed oscillations as a function of cluster size in phase with icosahedral geometric shell structure. As the temperature was raised, the oscillations disappeared starting from the smallest cluster sizes. The temperature at which the oscillation disappeared for a certain size region was interpreted as the melting temperature for that cluster size. Interestingly, the melting temperatures were found to increase only by 15 K as the particle number of the cluster increased from 923 to 10 179, and they did not seem to extrapolate to the bulk melting temperature as a function of $N^{-1/3}$ as expected from theoretical considerations [3]. The weak size dependence suggested that surface melting was responsible for the observed smoothening of the mass spectrum.

Theoretically, the melting temperatures of metal clusters have usually been determined with classical molecular dynamics using "semiclassical" many-atom potentials of the embedded atom method (EAM), the effective medium theory (EMT) or the tight-binding (TB) approximation [3–7]. Several studies along these lines have been performed also for sodium clusters with less than 55 atoms [6,7]. Calvo and Spiegelmann studied melting of sodium clusters with 8–147 atoms using both semiclassical TB potentials and the true quantum mechanical TB method taking explicitly into account the electronic level structure [8]. None of these methods was able to produce the nonmonotonous size-dependence of the melting temperature observed experimentally [1].

Ab initio molecular dynamics methods, where the forces are determined from an electronic structure calculation, have been used to study the melting of sodium clusters only for clusters with less than 20 atoms [9] and for two special cases of larger clusters, Na_{40} [10] and Na_{55}^{+} [11]. In the case of $N = 55$, the theoretically estimated melting temperature, $310 \cdots 360$ K [11], is in fair agreement with the experimental result of 290 K [1]. For the smaller sizes, no experimental results exist.

Surface melting and its effect on electronic properties have not been studied theoretically in the case of sodium clusters. Molecular dynamics simulations for plane Cu surfaces [12] and for finite Cu clusters [3,13] suggest that surface melting is a common property of metal clusters. Also Lennard-Jones clusters have been observed to exhibit surface melting [13,14].

The purpose of the present paper is not to determine accurately the melting or surface melting temperature for

[a] e-mail: ar@phys.jyu.fi

clusters but to study the effect of melting transition on the ionization potential (*IP*) of the cluster. While the experiments of Schmidt *et al.* [1] do not rely directly on the ionization potential, the method used by Martin *et al.* [2] for large clusters do: they observed the melting by the change in the ionization potential. We determine the average ionization potential at different temperatures around the melting point and look for its correlation with the phase and the surface structure. For a detailed study we choose two cluster sizes $N = 142$ and $N = 147$, a nearly complete icosahedron and a complete icosahedron. For larger icosahedra, we use only a semiclassical method to study the possible surface melting.

The ionization potential of a finite metal sphere is expected to depend on its radius R as

$$IP(R) = W + \left(\frac{1}{2} + c\right)\frac{e^2}{R} + O(R^{-2}), \qquad (1)$$

where W is the bulk work function and $c \approx -0.08$ [15]. On top of this average behavior one finds oscillations which are caused in the case of small clusters by the electronic shell structure and deformation [16,17] and in the case of large clusters by the geometric shell structure [18]. For small sodium clusters, the ionization potential has been measured quite accurately [19,20]. Theoretical work was earlier limited to determining the adiabatic or vertical ionization potential for the ground state [21]. Only recently, *ab initio* molecular dynamics has been used to study the temperature dependence of the ionization potential of metal clusters [22–24]. In these studies, the photoionization efficiency (PIE) curves were estimated using the Kohn-Sham single-electron states extracted from *ab initio* molecular dynamics simulations. The theoretical PIE curves where then used to determine the *IP* at a certain temperature using similar methods as in experimental studies [24]. The calculations were based on the Generalized Koopman's theorem [25]

$$-IP(N) = \epsilon_{\mathrm{HOMO}}(N) - v_{xc}^{\infty}(N), \qquad (2)$$

where $\epsilon_{\mathrm{HOMO}}(N)$ is the energy of the highest occupied single-electron state and $v_{xc}^{\infty}(N)$ is the asymptotic limit of the exchange-correlation potential of a system with N electrons. In reference [23], the *IP* values calculated for Al_6 and Al_7 systematically showed a decreasing tendency as a function of temperature. In reference [24], the *IP* values were calculated for Na_8 to Na_{55} in the temperature region 200–350 K and compared with experimental findings obtained with different methods.

In this paper, the ionization potential of Na_{142} and Na_{147} as a function of temperature is studied directly, without equation (2), using an *ab initio* calculation method. The caloric curves for sodium clusters with from 142 to 1 415 atoms were determined using a semiclassical molecular dynamics simulation method. From the semiclassically determined trajectories, 10 atomic configurations were extracted for both Na_{142} and Na_{147} at three temperatures around the melting temperatures for these two cluster sizes. For these 60 atomic configurations, vertical ionization potentials were calculated using an *ab initio* method [26]. The vertical ionization potentials were also calculated for optimized, icosahedron-based structures for Na_{142} and Na_{147}.

The main results are as follows. (1) The semiclassical TB energies correlate roughly with the *ab initio* energies, but details of the ionic motion can not be determined with semiclassical methods. (2) Clusters with more than 300 atoms exhibit clear surface melting. Reconstruction of the surface layer starts at a temperature which seems to be nearly independent of the cluster size. (3) The ionization potential of the full icosahedron with 147 atoms is higher than that of the cluster with 142 atoms at zero temperature. However, when the temperature is increased close to the melting temperature the difference disappears. (4) The generalized Koopman's theorem is an accurate method for determining the ionization potential of sodium clusters in agreement with the findings of Akola *et al.* [24].

2 Simulation methods

Semiclassical molecular dynamics simulations were performed to determine the caloric curves of sodium clusters and to extract atomic configurations for the *ab initio* calculations of ionization potentials for Na_{142} and Na_{147}. The simulations were performed with a semiclassical many-body potential

$$V = \sum_{i=1}^{N}\left\{\sqrt{\sum_{j=1\neq i}^{N}\zeta_0^2 \exp\left[-2q\left(\frac{r_{ij}}{r_0}-1\right)\right]} - \sum_{j=1\neq i}^{N}\epsilon_0 \exp\left[-p\left(\frac{r_{ij}}{r_0}-1\right)\right]\right\} \qquad (3)$$

where $\epsilon_0 = 15.956$ meV, $\zeta_0 = 291.14$ meV, $r_0 = 6.99$ a_0, $q = 1.30$ and $p = 10.13$. This potential is based on the tight-binding approximation [27] and the parameterization used here is extracted from [28]. The Nosé-Hoover [29] thermostat was employed to keep the temperature fluctuating around the desired value. The time step used was 5 fs.

A series of constant-temperature simulations was performed for sodium clusters with 142, 147, 309, 923 and 1 415 atoms at a temperature region chosen for each cluster size to be around the melting temperature and at least 50 K wide. Each simulation was started from an icosahedral atomic configuration with the velocities corresponding to the Maxwell-Boltzmann distribution at the desired average temperature. For Na_{142}, the starting configuration was an icosahedron with 5 missing vertex atoms. Each cluster was first equilibrated for 0.9 ns and then data was collected for 5.0 ns. From the average potential energy values obtained using the data from the 5.0 nanosecond period for each temperature, caloric curves were constructed for each cluster size.

The melting temperature of the cluster means here the temperature at which the whole cluster becomes liquid. Melting was determined with help of the caloric curve

and confirmed by using various other indicators like mean square displacement, radial distribution function, liquid parameter and the percentage of configurations where an icosahedron was found inside the cluster. Details of the last two methods can be found in reference [14]. Surface melting was determined from the difference between the mean square displacement of the surface atoms and the rest of the atoms.

The vertical ionization potentials (*vIP*) for Na_{142} and Na_{147} were calculated by solving the Kohn–Sham (KS) one-electron equations for the single-electron states of the valence electrons for a given nuclear configuration of the ions, using the plane wave technique developed by Barnett and Landman [26]. The valence electron–ion interaction was presented with the norm-conserving, non-local, separable [30] pseudopotentials by Troullier and Martins [31], and the LSD parameterization was taken from reference [32]. A converged solution was calculated for both neutral and singly ionized cluster, and the vertical ionization potential was attained as the difference between the energy values obtained for these cases.

The ionization potential as a function of temperature was determined for atomic configurations extracted from the semiclassical molecular dynamics simulations described above. For each temperature studied, we used 10 configurations taken at instants of time from 0.48 ns to 4.80 ns at regular intervals of 0.48 ns. For the *ab initio* simulations, the ions were placed at the coordinates corresponding to these semiclassically determined atomic configurations. The converged solution for the electronic ground state energy was calculated for the fixed ionic configuration for both neutral and singly ionized cluster. The *IP* was determined as the difference of these two total energies. Finally, the ionization potential for each temperature and size was calculated as an average over the ones determined for the 10 ionic configurations.

The *vIP*'s were also calculated for the icosahedron-based Na_{142} and Na_{147} (ground state) geometries, which were optimized using the *ab initio* method. The resulted optimized structures are local minima closest to the starting configurations, and no further optimizations were performed. The electronic temperature was kept at the same value as the kinetic temperature of the semiclassical simulation for each cluster except for the optimized structures, for which an electronic temperature of 120 K was employed to ensure convergence.

3 Results and discussion

3.1 Melting and surface melting

Constant-temperature molecular dynamics simulations revealed qualitatively different melting behavior for the smallest and the largest clusters studied. For large clusters, Na_{923} and Na_{1415}, the surface of the cluster could be interpreted liquid by all indicators used, already at temperatures more than 20 K below the theoretical melting temperature of the cluster. The number of mobile atoms increased as a function of temperature starting from the surface until the whole cluster melted. For Na_{142} and Na_{147}, however, coexistence of solid and liquid phases was found and no evidence of surface melting was shown by the indicators employed. For Na_{309}, both phase coexistence and surface melting were found, but not as clearly as for the other sizes. For comparison, Lennard-Jones clusters with 100, 200, and 400 atoms, simulated in vapor, showed no clear signs of phase coexistence, but surface melting was detected for each cluster size [14]. Surface melting was also studied in reference [13].

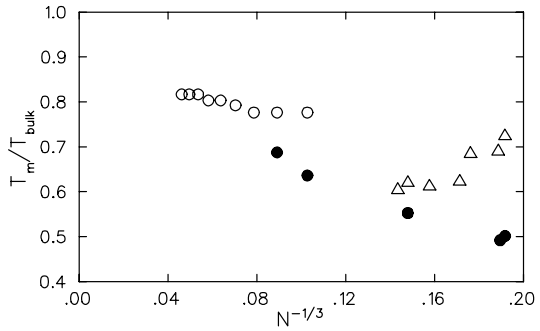

Fig. 1. Melting temperature (the temperature where the whole cluster melts) of sodium clusters as a function of size, scaled to the experimental bulk melting temperature. The closed symbols represent the semiclassical molecular dynamics simulation results determined here. The open circles represent the experimental results of reference [2] and the open triangles the ones of reference [1].

Figure 1 shows the melting temperatures (the temperature where the whole cluster melts) obtained with the semiclassical many-body potential of equation (1) for sodium clusters with 142, 147, 309, 923, and 1 415 atoms. The melting temperatures obtained follow the law $T_m = AN^{-1/3}$ given by the liquid drop model and approach the bulk melting temperature as the cluster size increases. The calculated value for the bulk melting temperature of the model potential used is 333 K. Note however, that the results shown in Figure 1 are scaled to the experimental melting temperature of the bulk sodium, 371 K.

Comparing with the experimental results of Martin *et al.* [2] also shown in Figure 1, one notes that there is a relatively large discrepancy of approximately 50 K between the experimental and simulation results for clusters with 923 and 1 415 atoms for which both results exist. The interpretation that the experimental results are caused by surface melting would make the discrepancy even bigger.

Figure 1 also shows a few experimental results by Schmidt *et al.* for smaller sodium clusters [1]. Also these do not agree with the numerical results calculated with the model of equation (3). For Na_{142}, the simulated melting temperature is approximately 80 K lower than the one determined experimentally by Schmidt *et al.*, and for Na_{309}, 25 K lower. However, our results agree with the Monte Carlo simulation results of Calvo and Spiegelmann [8] who found with an essentially similar potential the melting temperature of 240 K for Na_{147}. It is interesting to note that the melting temperature of 142 atoms obtained

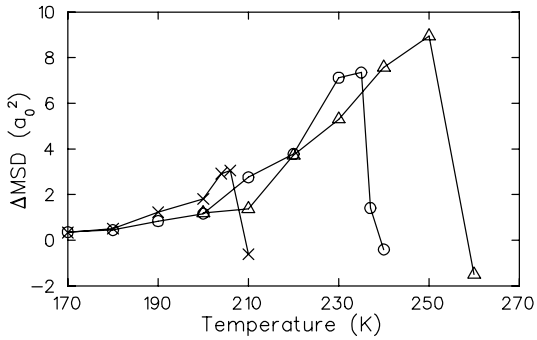

Fig. 2. Difference between the mean square displacement, calculated as an average over periods of 30 ps, for the surface atoms and for the rest of the atoms. The crosses, the open circles and the open triangles represent the results for Na_{309}, Na_{923} and Na_{1415}, respectively. A large value indicates surface melting and an abrupt decrease of the value to zero melting of the whole cluster.

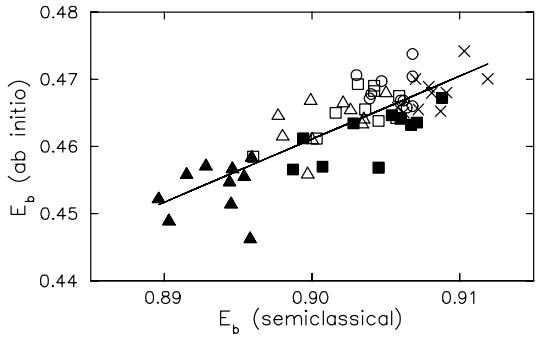

Fig. 3. Binding energy of Na_{142} and Na_{147} configurations calculated with the *ab initio* method as a function of the one calculated with the semiclassical method. The open circles, squares and triangles represent the results for Na_{142} at 160 K, 170 K and 185 K, respectively, and the crosses, the closed squares and the closed triangles the corresponding results for Na_{147}.

here is *higher* than that of the complete icosahedron, in agreement with the results of Schmidt *et al.* [1].

Figure 2 shows the difference between the mean square displacement of the surface atoms (the outermost icosahedral shell) and the rest of the atoms for cluster sizes 309, 923, and 1 415. The bulk melting is seen as a sudden disappearance of the difference, and it happens clearly at different temperatures for different cluster sizes. Before the bulk melting the difference curves follow closely to each other, indicating that surface melting starts roughly at the same temperature, at about 200 K. This is in qualitative agreement with the results of Martin *et al.* [2] shown in Figure 1, but our estimate for the temperature of the surface melting is much too low as compared to the experimental results.

3.2 Ionization potential

The vertical ionization potential was calculated using the *ab initio* LDA method for sodium clusters with 142 and 147 atoms. The temperature region was chosen on the basis of the caloric curves obtained with the semiclassical simulations. For Na_{147}, the configurations correspond to solid structures at 160 K, both solid and liquid structures at 170 K, and liquid structures at 185 K. For Na_{142}, the semiclassical potential gives somewhat higher melting temperature and the configurations correspond to solid structures at 160 K, and both solid and liquid structures at 170 K and 185 K.

It is by no means clear that the sampling of the phase space based on the semiclassical potential is realistic for studying the temperature dependence of the ionization potential. Figure 3 shows, however, that there is a correlation between the potential energy given by the semiclassical model and the total energy given by the LDA calculation. The fitted linear dependence (solid line) has a slope of 0.9. Note that the *ab initio* values are shifted because of the use of the LDA energy value for the sodium atom. Nevertheless, the scattering of the data and the correlation

Table 1. Correlation of the vertical ionization potential with different variables. The correlation coefficient is calculated using for each cluster size 30 points calculated at temperatures 160, 170 and 185 K (ten points in each). E_b(TB) and E_0(LDA) are the semiclassical potential energy and the *ab initio* total energy, ϵ_{HOMO} is the energy of the highest molecular orbital, and $r_{\max}(i)$ is the average distance of i outermost atoms of the cluster. The last row shows the correlation coefficient between the semiclassical and *ab initio* energies.

Correlation	Na_{142}	Na_{147}
vIP / $-E_b$(TB)	0.03	0.83
vIP / $-E_0$(LDA)	0.06	0.75
vIP / $-\epsilon_{\mathrm{HOMO}}$	0.93	0.99
vIP / $r_{\max}(1)$	−0.49	−0.13
vIP / $r_{\max}(10)$	−0.22	0.10
vIP / $r_{\max}(1) - r_{\max}(85)$	−0.52	0.05
$-E_b$(TB) / $-E_0$(LDA)	0.66	0.89

coefficients (the last line in Tab. 1) reveal that while the energies calculated with different methods have roughly the same variation at a given temperature, they are not very well correlated. This is a strong indication that the electronic structure still has a marked effect on the total energy for cluster sizes around 150 atoms.

For comparison, the *vIP* values were calculated also for optimized Na_{142} and Na_{147} structures. For Na_{147}, in *ab initio* calculations the icosahedron was found to lie 2.50 eV lower in energy than the cuboctahedron, and was chosen for the *vIP* calculation. For Na_{142}, the optimized structure is based on the icosahedron with missing vertex atoms.

Figure 4 shows the vertical ionization potential of Na_{142} and Na_{147} as a function of temperature determined with *ab initio* calculations using the atomic configurations extracted from the semiclassical molecular dynamics simulations. For comparison, the *vIP* values were calculated also for optimized (zero temperature) structures for Na_{142} and Na_{147}. All points, except for the optimized structures, represent an average over 10 configurations extracted from the semiclassical simulation for a particular size and

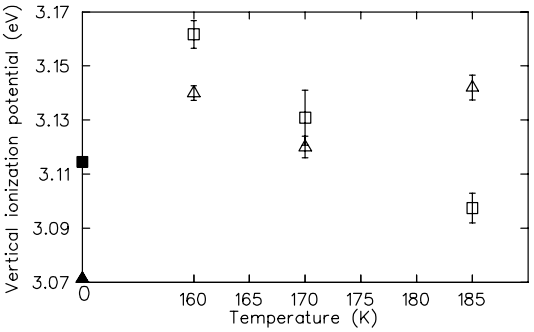

Fig. 4. Vertical ionization potential from the *ab initio* calculations as a function of temperature. The triangles and the squares represent averages over 10 configurations for Na_{142} and Na_{147}, respectively. The closed symbols represent the results for optimized, icosahedron-based configurations. The error bars represent the standard deviation of the mean over 10 configurations.

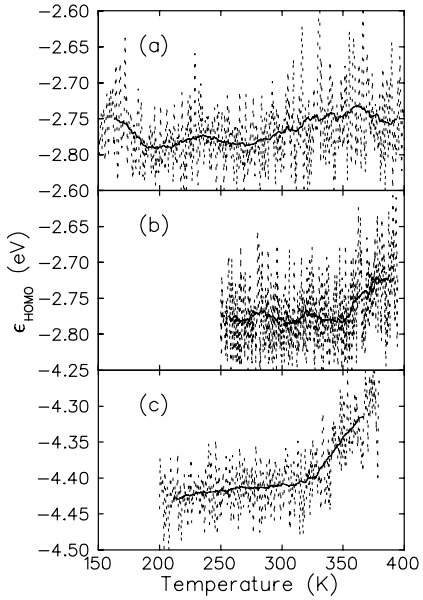

Fig. 5. The energy of the highest occupied Kohn-Sham single-electron state for (a) Na_{40} heated at 5 K/ps, (b) Na_{40} heated at 2.5 K/ps, and (c) Na_{55}^{+} heated at 5 K/ps. The solid line gives an average of the curve over a time window of 5.0 ps. The data is extracted from references [10,11].

temperature. For both cluster sizes, the ionization potential increases when the temperature is increased from zero. At the melting region, the *vIP* of Na_{147} decreases clearly while that of Na_{142} seems to be less dependent on the temperature. The large difference of *vIP* at zero temperature diminishes when the temperature is increased to 160 K, *i.e.* clearly below the melting temperature. At the highest temperature studied (185 K), Na_{142} has a higher *vIP* than Na_{147}.

Decreasing of *vIP* as a function of temperature has been observed before in *ab initio* calculations of small sodium clusters [24] and also for Al_6 and Al_7 [23]. When observed in the melting region, this behavior is consistent with the experimental observation that for close-packed structures, the ionization energy is higher than for sizes between the magic numbers [18]. This would indicate that for non-close-packed structures, the ionization potential should be lower than for close-packed ones. The stability of the structure is generally believed to correlate with the *IP*. Following this picture, one would expect *vIP* to decrease when the temperature is increased. Figure 4 shows that the situation is more complicated. One should note, however, that at a finite temperature the value of the *IP* depends on its detailed definition [24].

Table 1 shows correlations of the *vIP* to different properties of the clusters. The first notion is that the *vIP* correlates very well with the energy eigenvalue of the highest occupied molecular orbital (HOMO). This means that *vIP* can be reliably determined with the Generalized Koopman's theorem (Eq. (2)). It also seems to indicate that the asymptotic exchange-correlation energy for a given cluster size is independent of the geometry. On the other hand, the *vIP* does not correlate well with the total energy of the cluster.

In large clusters, the ionization potential is expected to depend on the detailed structure of the surface, in the same way as the work function of a metal depends on the roughness of the surface [33]. Normally, the roughness is determined as the height-height correlation function [34]. In a small cluster, it is difficult to quantify the roughness but the surface height can be measured from the center of mass of the cluster. We define $r_{\max}(n)$ to be the average distance of the n outermost atoms from the center of mass. In Table 1 we give the correlation factors determined with help of $r_{\max}(n)$. The first is simply the distance of the outermost atom and the second the average distance of the 10 outermost atoms. These two will be increased not only by surface fluctuations but also by, for example, an overall quadrupole deformation of the whole cluster. That is why we also determined the correlation of *vIP* with $r_{\max}(1) - r_{\max}(85)$, which measures perhaps better the local roughening of the surface since the average distance of the outermost atomic layer is substracted. There seems not to be any clear correlation between the detailed surface roughness and the *vIP*. This is quite surprising, since the *vIP* at high temperature is anyway different from the zero temperature values.

For each of the 60 atomic configurations studied, it was also investigated if the size of the perfect icosahedron found inside the cluster (147, 55, 13, or 0) would correlate with the *vIP* calculated for that atomic configuration. These were compared with bare eye because for these quantities, the correlation coefficient is not a good quantity. Also for this case, no correlation was found.

Because the *vIP* was found to correlate well with $-\epsilon_{\mathrm{HOMO}}$, the dependence of the ionization potential on the phase of the cluster can also be studied by examining ϵ_{HOMO} as a function of the phase of the cluster. Figure 5 shows ϵ_{HOMO} as a function of temperature obtained from three simulations for Na_{40} and Na_{55}^{+}. The data shown in Figure 5 is extracted from references [10,11]. For each case, ϵ_{HOMO} shows an average increase at the same

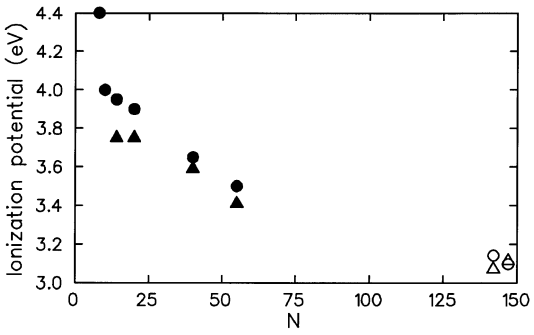

Fig. 6. Ionization potential of sodium clusters as a function of N. The open symbols represent the results obtained here; the triangles for the optimized structures and the circles for structures at 185 K. The closed symbols represent results obtained with the baseline intercept method; experimental results at less than 100 K (triangles) [20] and *ab initio* simulation results at 200 K (circles) [24].

temperature region where melting was detected from the caloric curve (300 K for Na_{40} heated at a constant rate of 5 K/ps, 350 K for Na_{40} heated at 2.5 K/ps, and 310–360 K for Na_{55}^+ heated at 5 K/ps). The magnitude of the increase is of the order of 0.05 to 0.1 eV, which is of the same order of magnitude as the variation of the *IP* values near the melting region for Na_{142} and Na_{147} shown in Figure 4. The scatter of the ϵ_{HOMO} values is, however, of the order of 0.20 eV. This seems to indicate that the ionization potential of a cluster depends strongly on its atomic configuration, and good statistics of results is required to get an accurate average value of *IP* for a certain cluster size at a certain temperature.

Figure 6 shows the calculated *IP* for sodium clusters in comparison with earlier theoretical [24] and experimental [20] results for small clusters. The overall energy region of the *vIP* values obtained here is consistent with earlier *IP* determinations and follows nicely the asymptotic dependence curve of equation (1).

Considering the results of Martin *et al.* [2], our results would indicate that the observed smoothening of the mass spectra curves is not necessarily due to the bulk or surface melting of the clusters. Our results show a gradual change of *vIP* as a function of temperature, but no abrupt changes were found as the cluster configuration was changed from ordered to disordered state. Remember, however, that the temperatures where Martin *et al.* [2] found the transition are much higher than the melting temperatures found in our semiclassical simulations (see Fig. 1).

It is relevant to ask if the fact that the configurations are taken from semiclassical simulations affects our conclusions. Provided that the icosahedron based structures are the energetically most favorable ones in this size region, the atomic configurations used here are realistic. There is strong evidence, both numerical [24] and experimental [35], that the (slightly distorted) icosahedron is the ground state structure for Na_{55}. Also in our calculations, the icosahedron was found to be lower in energy than cuboctahedron for Na_{147}. For liquid structures, the situation is different because our semiclassical structures are not deformed. For example, there is evidence that during the melting transition, the electronic structure of Na_{55}^+ loses almost completely its spherical jellium type characteristics and examining the principal moments of inertia, one finds that the cluster becomes clearly prolate [11]. However, the lack of correlation between *vIP* and $r_{\max}(1)$ or $r_{\max}(10)$ suggests that the *vIP* may not be significantly affected by quadrupole deformation of the cluster.

4 Summary

We have performed both *ab initio* and semiclassical simulations with a many-atom potential on melting and phase dependence of the ionization potential of large sodium clusters. We found that for the semiclassical model used, the melting temperatures approach the bulk value linearly as a function of $N^{-1/3}$ for the size region 142–1 415. For $N = 923$ and 1 415, the values given by the model are at least 30 to 50 K lower than the experimental estimates [2]. The vertical ionization potential calculated correlates with the energy of the highest occupied electronic state in accord with the Generalized Koopman's theorem, but does not correlate with either the surface disorder, the geometrical binding energy, or the total energy given by the *ab initio* calculation.

We wish to thank H. Häkkinen for valuable discussions. This work has been supported by the Academy of Finland under the Finnish Centre of Excellence Programme 2000-2005 (Project No. 44875, Nuclear and Condensed Matter Programme at JYFL).

References

1. M. Schmidt, R. Kusche, W. Kronmüller, B. von Issendorff, H. Haberland, Phys. Rev. Lett. **79**, 99 (1997); R. Kusche, Th. Hippler, M. Schmidt, B. von Issendorff, H. Haberland, Eur. Phys. J. D **9**, 1 (2000); M. Schmidt *et al.*, in *The Physics and Chemistry of Clusters*, Proceedings of Nobel Symposium 117 (World Scientific, Singapore, 2001), p. 326
2. T.P. Martin, U. Näher, H. Schaber, U. Zimmermann, J. Chem. Phys. **100**, 2322 (1994)
3. S. Valkealahti, M. Manninen, Comp. Mater. Sci. **1**, 123 (1993)
4. C.L. Cleveland, W.D. Luedtke, U. Landman, Phys. Rev. Lett. **81**, 2036 (1998)
5. H. Grönbeck, D. Tománek, S.G. Kim, A. Rosen, Z. Phys. D **40**, 469 (1997)
6. R. Poteau, F. Spiegelmann, P. Labastie, Z. Phys. D **30**, 57 (1994)
7. N. Ju, A. Bulgac, Phys. Rev. B **48**, 2721 (1993)
8. F. Calvo, F. Spiegelmann, J. Chem. Phys. **112**, 2888 (2000)
9. U. Röthlisberger, W. Andreoni, J. Chem. Phys. **94**, 8129 (1991)
10. A. Rytkönen, H. Häkkinen, M. Manninen, Phys. Rev. Lett. **80**, 3940 (1998)
11. A. Rytkönen, H. Häkkinen, M. Manninen, Eur. Phys. J. D **9**, 451 (1999)

12. H. Häkkinen, M. Manninen, Phys. Rev. B **46**, 1725 (1992)
13. H.-P. Cheng, R.S. Berry, Phys. Rev. A **45**, 7969 (1992)
14. A. Rytkönen, S. Valkealahti, M. Manninen, J. Chem. Phys. **108**, 5826 (1998)
15. M. Seidl, J.P. Perdew, Phys. Rev. B **50**, 5744 (1994)
16. E.C. Honea, M.L. Homer, J.L. Persson, R.L. Whetten, Chem. Phys. Lett. **171**, 147 (1990)
17. W.A. de Heer, Rev. Mod. Phys. **65**, 611 (1993)
18. T.P. Martin, T. Bergmann, H. Göhlich, T. Lange, J. Phys. Chem. **95**, 6421 (1991)
19. M.M. Kappes, M. Schär, U. Röthlisberger, C. Yeretzian, E. Schumacher, Chem. Phys. Lett. **143**, 251 (1988)
20. M.L. Homer, J.L. Persson, E.C. Honea, R.L. Whetten, Z. Phys. D **22**, 441 (1991)
21. V. Bonačić-Koutecký, P. Fantucci, J. Koutecký, Phys. Rev. B **37**, 4369 (1988)
22. J. Akola, H. Häkkinen, M. Manninen, Phys. Rev. B **58**, 3601 (1998)
23. J. Akola, H. Häkkinen, M. Manninen, Eur. Phys. J. D **9**, 179 (1999)
24. J. Akola, A. Rytkönen, H. Häkkinen, M. Manninen, Eur. Phys. J. D **8**, 93 (2000)
25. D.J. Tozer, N.C. Handy, J. Chem. Phys. **108**, 2545 (1998); *ibid.* **109**, 10180 (1998)
26. R.N. Barnett, U. Landman, Phys. Rev. B **48**, 2081 (1993)
27. D. Tomanék, S. Mukherjee, K.H. Bennemann, Phys. Rev. B **28**, 665 (1983)
28. Y. Li, E. Blaisten-Barojas, D.A. Papaconstantopoulos, Phys. Rev. B **57**, 15519 (1998)
29. S. Nosé, Mol. Phys. **52**, 255 (1984); W.G. Hoover, Phys. Rev. A **31**, 1695 (1985)
30. L. Kleinman, D.M. Bylander, Phys. Rev. Lett. **48**, 1425 (1982)
31. N. Troullier, J.L. Martins, Phys. Rev. B **43**, 1993 (1991)
32. S.H. Vosko, L. Wilk, M. Nusair, Can. J. Phys. **58**, 1200 (1980); S.H. Vosko, L. Wilk, J. Phys. C **15**, 2139 (1982)
33. A. Zangwill, *Physics of Surfaces* (Cambridge University Press, Cambridge, 1988)
34. J. Merikoski, H. Häkkinen, M. Manninen, J. Timonen, K. Kaski, Phys. Rev. B **49**, 4938 (1994)
35. G. Wrigge, M. Astruc Hoffmann, B. von Issendorff, Phys. Rev. A **65**, 63201 (2002)